Proper Elements for Space Debris and Applications

Tudor Vartolomei
Department of Mathematics, University Alexandru Ioan Cuza
Joint work with: Prof. Alessandra Celletti, Prof. Giuseppe Pucacco and Anargyros Dogkas

Scientific Seminar of the Astronomical Institute
11 October 2023

Table of Contents

Table of Contents

Real World Problem

Tracking and categorizing the space debris, with known and unknown origin, generated after a catastrophic event.

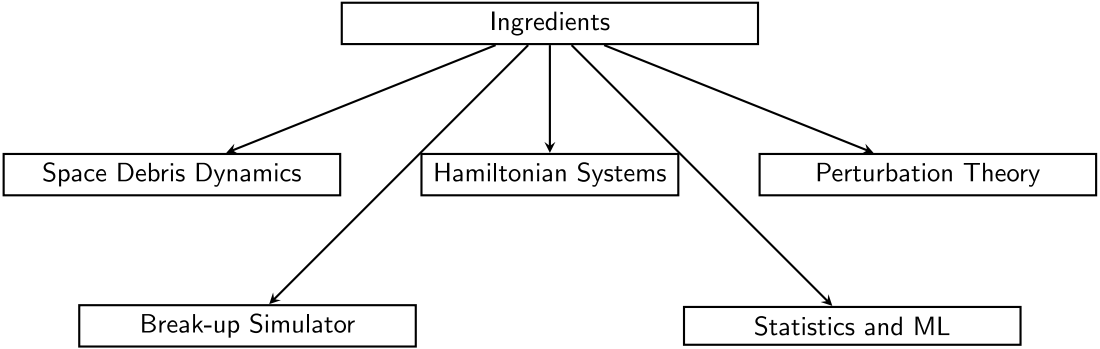

A Real-World Problem, State-of-the-Art and Overview

Space Debris Dynamics

What we know:

- Force model: Earth, Moon, Sun, Solar radiation pressure
- Initial conditions: observations

Problems:

- Approximate the real trajectories
- Errors from the observations
- Millions of objects

Space Debris Statistics

Space Debris:

1. Artificial or non-operational objects in orbit around the Earth
2. $\approx$ 1 000 000 objects larger than 1 cm
3. $\approx$ 130 million objects larger than 1 mm

Catastrophic events:

1. Generated by break-up events: Explosion or Collision
2. More than 500 confirmed breakups since 1961
3. Each time an object breaks up, a debris cloud is formed

Credits: NASA

A Real-World Problem, State-of-the-Art and Overview

Set of elements:

1. Cartesian coordinates
2. Orbital elements
    - Osculating elements
    - Mean elements
    - **Proper elements**
3. Delaunay variables
4. Poincaré variables

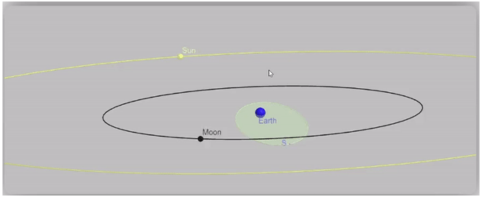

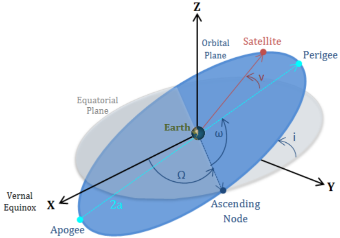

Credits: www.gsc-europa.eu

Dynamical system:

- **Newtonian approach**
- Lagrangian approach
- **Hamiltonian approach**

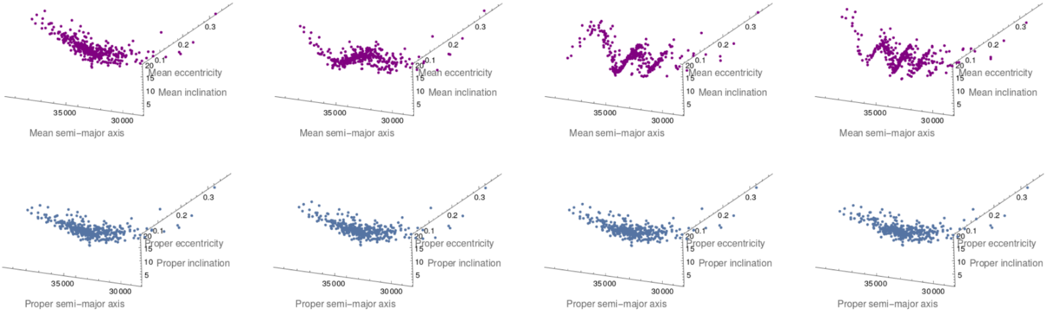

The evolution of the distribution of mean elements (upper plots) and proper elements (lower plots) over 180 years, at every 60 years in the 3-D coordinates a - e - i.

Table of Contents

A Model of Space Debris Dynamics

Reference systems:

- Earth Centered Inertial Frame (*ECIF*)
  - Origin = center of the Earth
  - Does not rotate with the Earth
  - X-axis = points to the vernal equinox direction
  - Z-axis = points to the North Pole direction
- J2000 system
  - ECIF
  - X-axis = aligned with the mean equinox (J2000.0, which is January 1, 2000 at 12:00)
- Synodic frame
  - Initial J2000
  - Rotating reference frame (by the angle θ around the axis of the Earth's rotation)

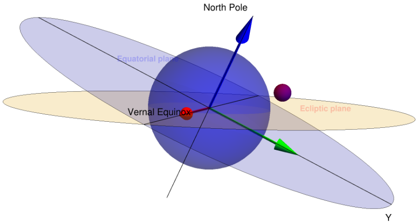

Quantity	Standard Units	Proper Units
1 second	$1s$	$\frac{2\pi}{86164.0905}$ pt
T_{SD}	$86164.0905\ s$	2π pt
R_E	≈ 6371 km	≈ 0.1511 pd
	$a_S \approx 149597870.691$ km	≈ 3547.99 pd
a_M	≈ 384400 km	≈ 9.1167 pd
μ_E	$398600.442\ \frac{km^3}{s^2}$	1 pu
μ_S	$132712440018\ \frac{km^3}{s^2}$	333060.4016 pu
μ_M	$4904.8695\ \frac{km^3}{s^2}$	0.0123 pu

A dynamical model of space debris

$$\mathcal{H} = \mathcal{H}_{Earth} - \mathcal{R}_{Moon} - \mathcal{R}_{Sun} + \mathcal{H}_{SRP} \tag{1}$$

- the Geopotential part (Kaula, 1962)

$$\mathcal{H}_{Earth} = -\frac{\mu_E}{a}\sum_{n=2}^{\infty}\sum_{m=0}^{n}(\frac{R_E}{a})^n\sum_{p=0}^{n}F_{nmp}(i)\sum_{q=-\infty}^{\infty}G_{npq}(e)S_{nmpq}(M,\omega,\Omega,\theta)$$

- the Moon perturbation (Kaula, 1966; Lane, 1989)

$$\begin{aligned}\mathcal{R}_{Moon} \quad &= Gm_M\sum_{l\geq 2}\sum_{m=0}^{l}\sum_{p=0}^{l}\sum_{s=0}^{l}\sum_{q=0}^{l}\sum_{j=-\infty}^{\infty}\sum_{r=-\infty}^{\infty}(-1)^{[m/2]}\frac{\epsilon_m\epsilon_s}{2a_M}\frac{(l-s)!}{(l+m)!}\left(\frac{a}{a_M}\right)^l F_{lmp}(i)\\ &F_{lsq}(i_M)H_{lpj}(e)G_{lqr}(e_M)\{(-1)^{t(m+s-1)+1}U_l^{m,-s}\cos(\phi_{lmpj}+\phi'_{lsqr}-y_s\pi)+\\ &(-1)^{t(m+s)}U_l^{m,-s}\cos(\phi_{lmpj}-\phi'_{lsqr}-y_s\pi)\}\end{aligned}$$

A dynamical model of space debris

- the Sun perturbation (Kaula, 1962)

$$\mathcal{R}_{Sun} = Gm_S \sum_{l\geq 2} \sum_{m=0}^{l} \sum_{p=0}^{l} \sum_{h=0}^{l} \sum_{q,j=-\infty}^{\infty} \frac{a^l \epsilon_m}{a_S^{l+1}} \frac{(l-m)!}{(l+m)!} F_{lmp}(i) F_{lmh}(i_S) H_{lpq}(e) G_{lhj}(e_S) \cos(\phi_{lmphqj})$$

- the Solar Radiation Pressure effect (Hughes, 1977)

$$\mathcal{H}_{SRP} = C_r P_r \frac{A}{m} a_S^2 \sum_{l=1}^{1} \sum_{s=0}^{l} \sum_{p=0}^{l} \sum_{h=0}^{l} \sum_{q=-\infty}^{\infty} \sum_{j=-\infty}^{\infty} \frac{a^l}{a_S^{l+1}} \epsilon_s \frac{(l-s)!}{(l+s)!} F_{lsp}(i) F_{lsh}(i_S) H_{lpq}(e) G_{lhj}(e_S) \cos(\phi_{lsphqj}) \ .$$

where C_r, P_r are, respectively, the reflectivity coefficient and the radiation pressure for an object located at $a_S = 1AU$, while $\frac{A}{m}$ denotes the area-to-mass ratio.

A Model of Space Debris Dynamics

Hamiltonian models:

Non-averaged model:

$$\mathcal{H}_{full}(\mathbf{oe}, \mathbf{oe}_M, \mathbf{oe}_S, \theta) = \mathcal{H}_{Kep}(\mathbf{oe}) + \mathcal{H}_E(\mathbf{oe}, \theta) + \mathcal{H}_M(\mathbf{oe}, \mathbf{oe}_M) + \mathcal{H}_S(\mathbf{oe}, \mathbf{oe}_S) + \mathcal{H}_{SRP}(\mathbf{oe}, \mathbf{oe}_S),$$

where $\mathbf{oe} = (a, e, i, M, \omega, \Omega)$, and subscripts S, M stand for Sun, and Moon respectively.

Doubly averaged model:

$$\begin{aligned}\mathcal{H}(e, i, i_M, a_S, \omega, \Omega, \Omega_M, M_S; a) &= \overline{\mathcal{H}_{J_2}}(e, i; a) + \overline{\mathcal{H}_{J_3}}(e, i, \omega; a) + \overline{\mathcal{H}_M}(e, i, i_M, \omega, \Omega, \Omega_M; a)\\ &+ \overline{\mathcal{H}_S}(e, i, \omega, \Omega; a) + \overline{\mathcal{H}_{SRP}}(e, i, a_S, \omega, \Omega, M_S; a)\end{aligned}$$

Resonant model:

$$\begin{aligned}\mathcal{H}_{resj:l}(e, i, i_M, a_S, \omega, \Omega, \Omega_M, M_S, \theta; a) &= \mathcal{H}_{Kep}(a) + \overline{\mathcal{H}_{J_2}}(e, i; a) + \overline{\mathcal{H}_{J_3}}(e, i, \omega; a) + \overline{\mathcal{H}_{resj:l}}(a, e, i, M, \omega, \Omega, \theta)\\ &+ \overline{\mathcal{H}_M}(e, i, i_M, \omega, \Omega, \Omega_M; a) + \overline{\mathcal{H}_S}(e, i, \omega, \Omega; a)\\ &+ \overline{\mathcal{H}_{SRP}}(e, i, a_S, \omega, \Omega, M_S; a)\end{aligned}$$

A Model of Space Debris Dynamics

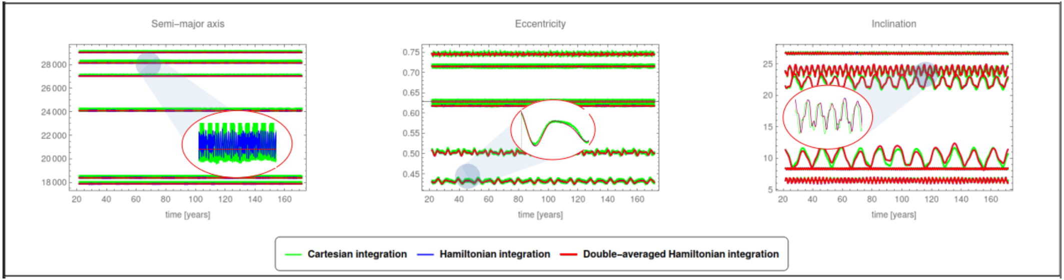

Comparison between the numerical integration of Cartesian equations of motion (green line), Hamilton's equations of the full Hamiltonian (blue line), Hamilton's equations of the doubly averaged Hamiltonian (red line).

Table of Contents

Perturbation theory - normal forms - theorem

Theorem

Let $(\boldsymbol{I}, \boldsymbol{\varphi}) \in B \times \mathbb{T}^n$ *be the action-angles variables, where* $B \subset \mathbb{R}^n$ *is an open set and* n *denotes the number of degrees of freedom, for a Hamiltonian function* $\mathcal{H} = \mathcal{H}(\boldsymbol{I}, \boldsymbol{\varphi})$ *defined by*

$$\mathcal{H}(\boldsymbol{I}, \boldsymbol{\varphi}) = \mathcal{H}_0(\boldsymbol{I}) + \varepsilon \mathcal{H}_1(\boldsymbol{I}, \boldsymbol{\varphi}) \ ,$$

where $\mathcal{H}_0(\boldsymbol{I})$ *represents the integrable part,* ε *is a small parameter and* $\mathcal{H}_1(\boldsymbol{I}, \boldsymbol{\varphi})$ *is a small perturbation, which is an analytic function on* $B \times \mathbb{T}^n$ *that can be written as:*

$$\mathcal{H}_1(\boldsymbol{I}, \boldsymbol{\varphi}) = \sum_{\boldsymbol{k} \in \mathcal{K}} b_{\boldsymbol{k}}(\boldsymbol{I}) \exp(i\boldsymbol{k} \cdot \boldsymbol{\varphi}).$$

If the frequency vector $\boldsymbol{\nu}$ *satisfies the non-resonance condition,* $|\boldsymbol{\nu}(\boldsymbol{I}_0) \cdot \boldsymbol{k}| > 0, \forall \boldsymbol{k} \in \mathcal{K}$, *and*$\forall \boldsymbol{I}_0 \in B$, *then there exists a canonical transformation* $(\boldsymbol{I}, \boldsymbol{\varphi}) \to (\boldsymbol{I}', \boldsymbol{\varphi}')$ *such that the Hamiltonian in the new variables becomes*

$$\mathcal{H}'(\boldsymbol{I}', \boldsymbol{\varphi}') = \mathcal{H}'_0(\boldsymbol{I}') + \varepsilon^2 \mathcal{H}'_1(\boldsymbol{I}', \boldsymbol{\varphi}').$$

Doubly averaged model:

$$\begin{aligned}\mathcal{H}(e,i,i_M,a_S,\omega,\Omega,\Omega_M,M_S;a) &= \overline{\mathcal{H}_{J_2}}(e,i;a)+\overline{\mathcal{H}_{J_3}}(e,i,\omega;a)+\overline{\mathcal{H}_M}(e,i,i_M,\omega,\Omega,\Omega_M;a\\ &+ \overline{\mathcal{H}_S}(e,i,\omega,\Omega;a)+\overline{\mathcal{H}_{SRP}}(e,i,a_S,\omega,\Omega,M_S;a)\end{aligned}$$

Delaunay variables:

$$\begin{aligned} l &= M & L &= \sqrt{\mu_E a}\\ g &= \omega & G &= \sqrt{\mu_E a(1-e^2)}\\ h &= \Omega & H &= \sqrt{\mu_E a(1-e^2)}\cos(i)\end{aligned}$$

Double-averaged Hamiltonian (Delaunay variables):

$$\begin{aligned}\mathcal{H}(g,h,h_M,l_S,G,H,H_M,L_S;L) &= \overline{\mathcal{H}_{J_2}}(G,H;L)+\overline{\mathcal{H}_{J_3}}(g,G,H;L)+\overline{\mathcal{H}_S}(g,h,G,H;L)\\ &+ \overline{\mathcal{H}_M}(g,h,h_M,G,H,H_M;L)+\overline{\mathcal{H}_{SRP}}(g,h,l_S,G,H,L_S;L)\end{aligned}$$

Perturbation theory - normal forms - iterative procedure

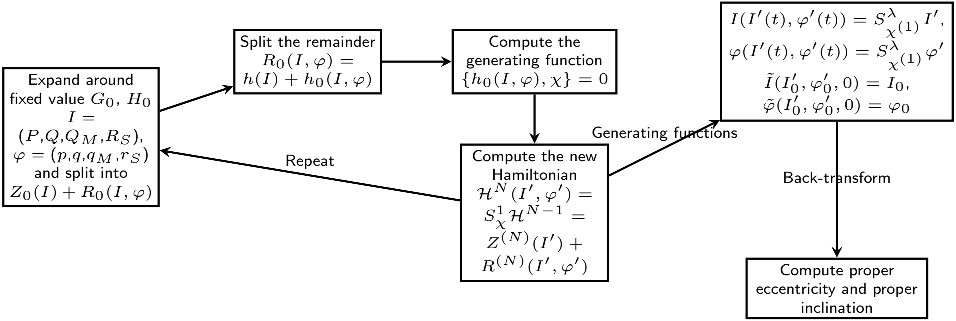

- Quasi-integrals of motion - nearly constant in time
- Kind of average signature of motion
- Identification of the spatial objects families (asteroids, space debris)
- The age and the origin of a space object

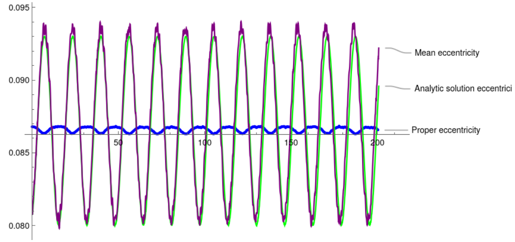

The evolution, over 200 years, of the mean eccentricity (purple lines), the analytic solution (green line) and the proper eccentricity (blue lines).

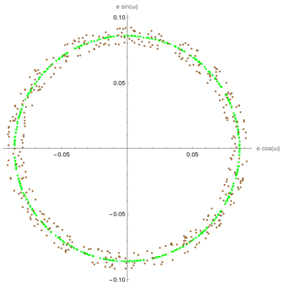

Mean elements (brown) and the proper elements (green) in Poincarè variables for $(e\cos(\omega), e\sin(\omega))$.

Initial conditions: $\{a, e, i, M, \omega, \Omega, A/m\}$=$\{11319.30\,km, 0.08, 19.84^\circ, 196.00^\circ, 243.85^\circ, 63.15^\circ, 0.34\,m^2/kg\}$.

Proper elements - higher-altitudes regions

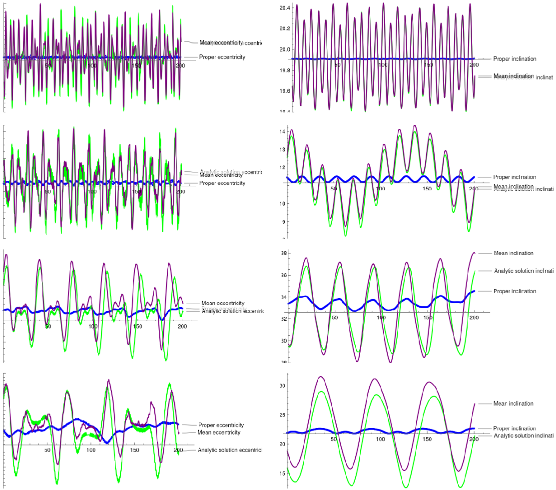

The evolution, over 200 years, of the mean elements (purple line), the proper elements (blue line) and the analytic solution (green line) of eccentricity (left) and inclination (right) with the initial conditions:

First line - $\{22493.3\,km, 0.19, 19.64°, 54.44°, 302.44°, 241.34°, 0.06\,m^2/kg\}$,

second line - $\{28138.5\,km, 0.16, 12.69°, 142.25°, 352.71°, 98.95°, 0.22\,m^2/kg\}$,

third line - $\{35611.2\,km, 0.29, 29.73°, 259.99°, 63.35°, 194.42°, 0.28\,m^2/kg\}$,

fourth line - $\{42683.0\,km, 0.07, 18.87°, 277.13°, 219.69°, 245.11°, 0.13\,m^2/kg\}$.

Proper elements - nearby orbits

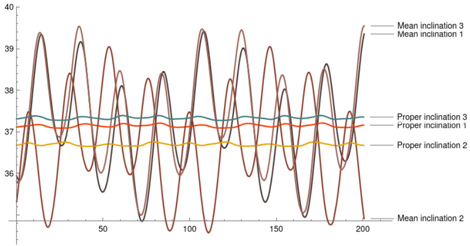

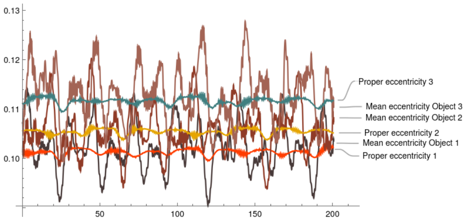

The evolution, over 200 years, of the mean elements (Brown colors) and the proper elements (Orange, Red, Green colors) of eccentricity (left) and inclination (right) for 3 different objects with the initial conditions:
$\{a, e, i, M, \omega, \Omega, A/m\}$=$\{29130\,km, 0.107, 35.94°, 62.36°, 44.14°, 212.17°, 0.67\,m^2/kg\}$
$\{a, e, i, M, \omega, \Omega, A/m\}$=$\{29074.3\,km, 0.101, 35.32°, 359.38°, 241.68°, 106.95°, 1.13\,m^2/kg\}$
$\{a, e, i, M, \omega, \Omega, A/m\}$=$\{29130.9\,km, 0.107, 35.80°, 4.402°, 20.41°, 198.09°, 1.47\,m^2/kg\}$.

Table of Contents

SIMPRO - Space Debris SIMulator and PROpagator

Break-up Simulator and Orbit Propagator

SIMPRO* - Simulator and propagator of space debris

Simulator - generate fragments after a collisions/explosions on the basis of the break-up model Evolve 4.0 provided by NASA:

Input:

- Mass / characteristic length of the generated fragment
- Mass & type of the parent object
- Mass of the small object
- Impact velocity

Output:

- Size of each generated fragment
- Area-to-mass of each fragment
- Ejection velocity of each generated fragment

***Joint work M. Apetrii, A. Celletti, C. Efthymiopoulos, C. Gales, T. Vartolomei**

STARDUST

PUSHING THE BOUNDARIES OF SPACE RESEARCH TO SAVE OUR FUTURE

Università di Roma Tor Vergata

MARIE CURIE ACTIONS

SIMPRO - Space Debris SIMulator and PROpagator

Break-up Simulator and Orbit Propagator

SIMPRO* - Simulator and propagator of space debris

- Explosion / Collision
- Characteristics of objects (mass, type, velocity)
- Output 1: a vs e, a vs i, and e vs i plots fragments generated
- Output 2: Statistics of the break-up
- Output 3: 3D visualization of the fragments (and evolution)
- Output 4: Distribution of orbital elements w.r.t. the size
- Output 5: Fragments generated (state vector and orbital elements)

- Input: mean elments / TLE
- Select the model (J2, J3, Moon, Sun, SRP, Drag effect)
- Choose the equations of motions (Hamiltonian / Cartesian / SGP4 / comparisons)
- Set the parameters (period[years/days] and step[hours/minutes])
- Integration method: Runge-Kutta / Adams-Bashfort-Multon
- Output: Evolution of orbital elements

SIMPRO* - Simulator and propagator of space debris

- Explosion / Collision
- Characteristics of objects (mass, type, velocity)
- Output 1: a vs e, a vs i, and e vs i plots fragments generated
- Output 2: Statistics of the break-up
- Output 3: 3D visualization of the fragments (and evolution)
- Output 4: Distribution of orbital elements w.r.t. the size
- Output 5: Fragments generated (state vector and orbital elements)

- Input: mean elments / TLE
- Select the model (J2, J3, Moon, Sun, SRP, Drag effect)
- Choose the equations of motions (Hamiltonian / Cartesian / SGP4 / comparisons)
- Set the parameters (period[years/days] and step[hours/minutes])
- Integration method: Runge-Kutta / Adams-Bashfort-Multon
- Output: Evolution of orbital elements

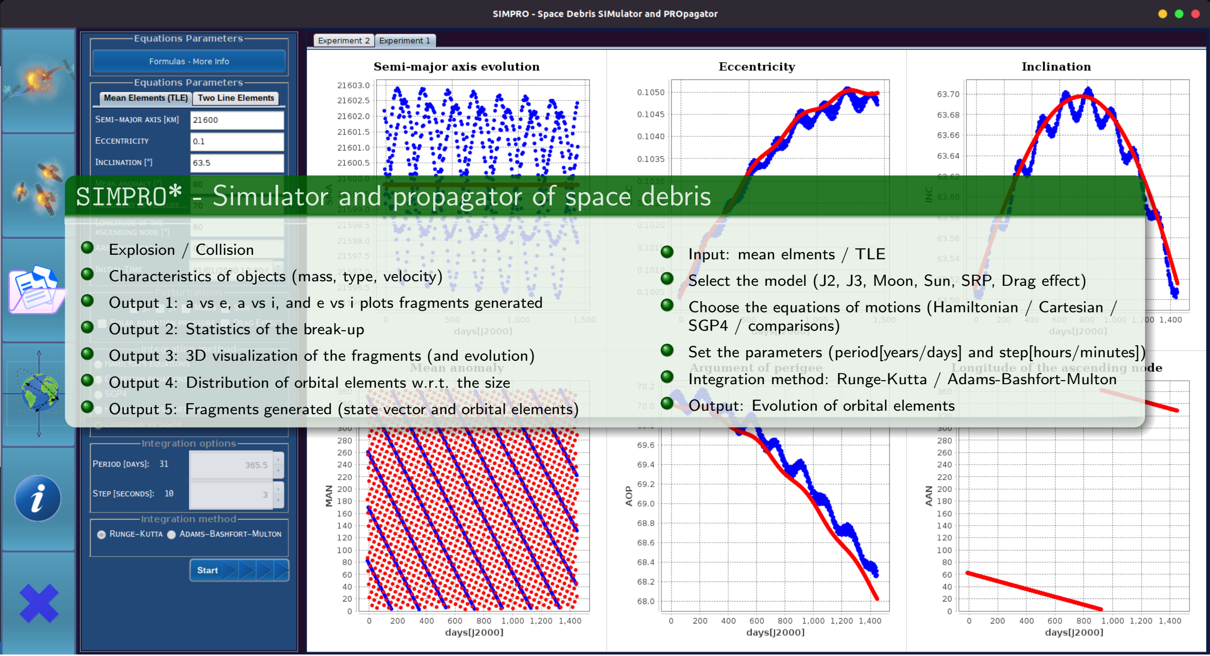

Simulations and results - single break-up event

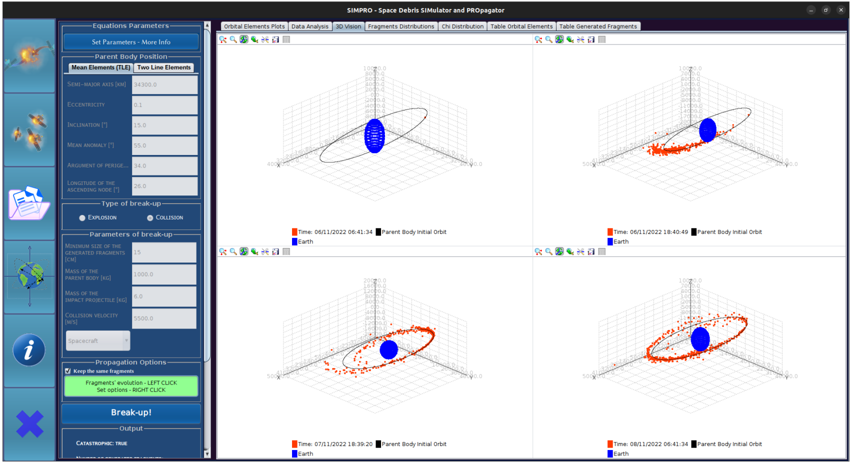

The evolution of group of the fragments over 2 days, at at every 12 hours in the 3-D Cartesian coordinates for the fragments generated by a collision between a spacecraft $(\{a, e, i, M, \omega, \Omega\} = \{34300\,km, 0.1, 15°, 55°, 34°, 26°\})$ of 1000 kg and a projectile of 6 kg at a velocity of 5500 m/s.

Simulations and results - single break-up event

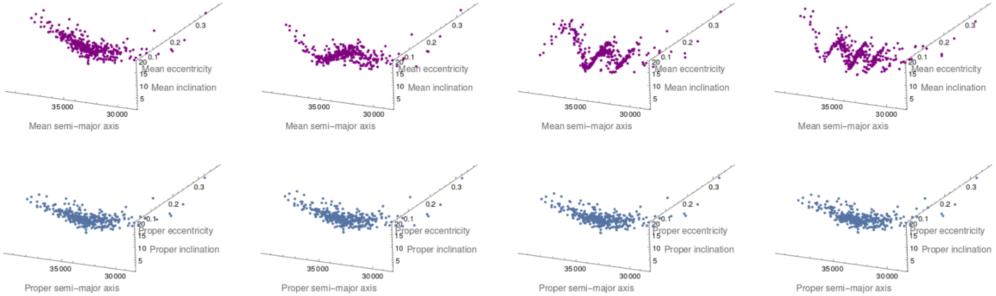

The evolution of the distribution of mean elements (upper plots) and proper elements (lower plots) over 180 years, at every 60 years in the 3-D coordinates a - e - i for the fragments generated by a collision between a spacecraft $(\{a, e, i, M, \omega, \Omega\} = \{34300\,km, 0.1, 15°, 55°, 34°, 26°\})$ of 1000 kg and a projectile of 6 kg at a velocity of 5500 m/s.

Simulations and results - single break-up event

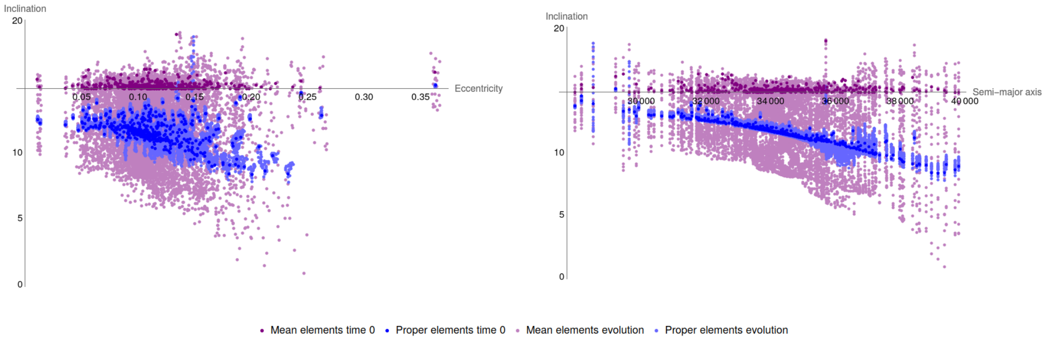

The comparison between variation of mean elements (purple and light purple dots) and proper elements (blue and light blue dots) for the fragments generated by a collision between a spacecraft ($\{a, e, i, M, \omega, \Omega\} = \{34300\,km, 0.1, 15°, 55°, 34°, 26°\}$) of 1000 kg and a projectile of 6 kg at a velocity of 5500 m/s.

Simulations and results - single break-up event

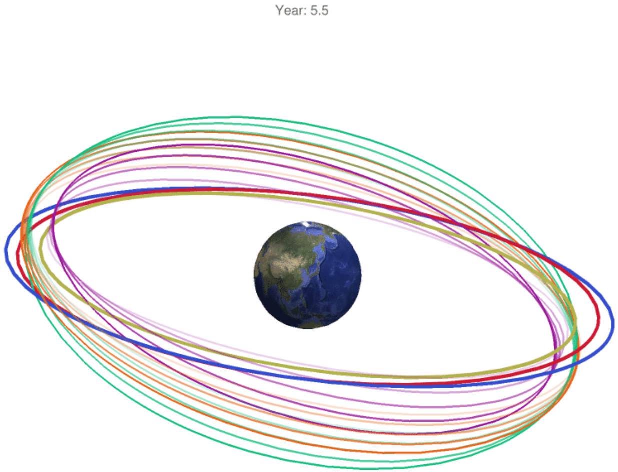

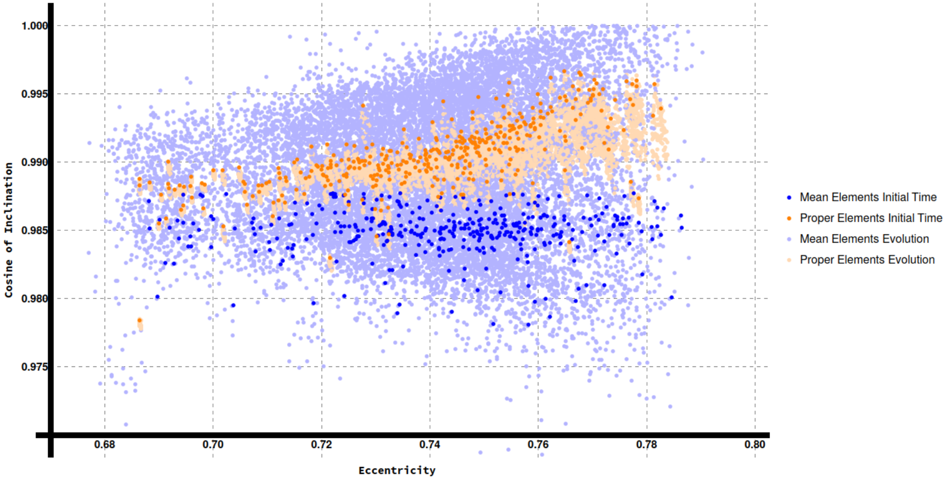

The comparison between variation of mean elements (purple and light purple dots) and proper elements (blue and light blue dots) for the fragments generated by a collision between a spacecraft ($\{a, e, i, M, \omega, \Omega\} = \{37600\,km, 0.75, 10°, 10°, 35°, 45°\}$).

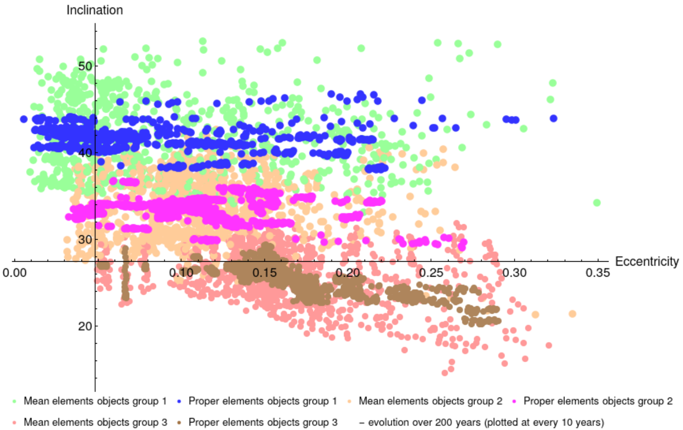

The comparison between the variation of the mean elements (group 1 - light green, group 2 - light orange, group 3 - light pink) and proper elements (group 1 - blue, group 2 - magenta, group 3 - brown) over 200 years, with the dots plotted every 10 years.

Simulations and results - three nearby groups

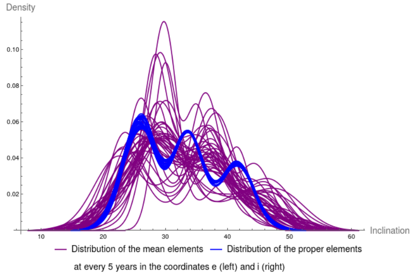

The probability density functions computed every 5 years, over 200 years, for the mean (purple lines) and proper (blue lines) inclination.

A mixture of three normal distributions (initial mean inclination):

$$0.41\,\mathcal{N}(29.8, 0.87){+}0.31\,\mathcal{N}(34.9, 1.09){+}0.27\,\mathcal{N}(41.3, 1.98)$$

A mixture of three normal distributions (initial proper inclination):

$$0.42\,\mathcal{N}(25.7, 1.91){+}0.31\,\mathcal{N}(33.4, 1.06){+}0.25\,\mathcal{N}(41.4, 1.75)$$

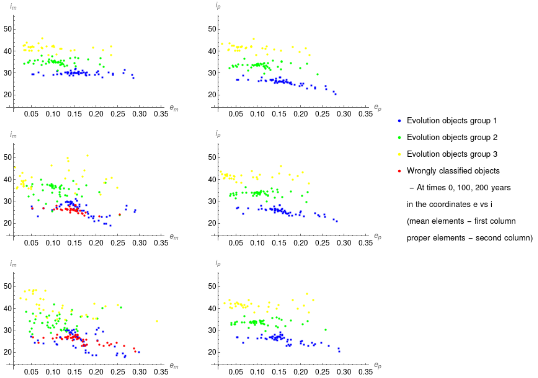

1. we separate the groups, both in the initial mean elements and initial proper elements at time T_0, and record the results;
2. at every intermediate time T_i, we use KMeans to classify the data in 3 groups and compare the original groups at time T_0 with the groups obtained at time T_i.
3. we plot with red dots the wrongly classified objects, namely the points for which the number (group) obtained at time T_i does not coincide with the number (group) obtained at the beginning, time T_0.

Table of Contents

On-going and future work:

- Analytical stability estimates, e.g. through higher-order normalization
- Computation of proper elements for space debris in LEO, namely including dissipative effects (with A. Celletti, C. Galeș, C. Lothka)
- Computation of proper elements for space debris in resonant regions (with A. Dogkas)
- Noise analysis by statistical methods and machine learning algorithms
- Synthetic proper elements

References

1. T. Vartolomei, Perturbative Methods and Proper Elements for the Satellite and Space Debris Problem, PhD Thesis (2023)
2. Alessandra Celletti, Anargyros Dogkas, Tudor Vartolomei, Dynamics of highly eccentric and highly inclined space debris, Communications in Nonlinear Science and Numerical Simulation, Volume 127, 2023, 107556, ISSN 1007-5704, https://doi.org/10.1016/j.cnsns.2023.107556.
3. Celletti, A., Pucacco, G. and Vartolomei, T. Reconnecting groups of space debris to their parent body through proper elements. Sci Rep 11, 22676 (2021). https://doi.org/10.1038/s41598-021-02010-x
4. Celletti, A., Pucacco, G. and Vartolomei, T. Proper elements for space debris. Celest Mech Dyn Astr 134, 11 (2022). https://doi.org/10.1007/s10569-022-10064-w
5. Celletti, A., Vartolomei, T. Old perturbative methods for a new problem in Celestial Mechanics: the space debris dynamics. Boll Unione Mat Ital (2023). https://doi.org/10.1007/s40574-023-00347-x
6. Celletti, A., Pucacco, G., and Vartolomei, T. (2019). Back-tracing space debris using proper elements. Proceedings of the International Astronomical Union, 15(S364), 134-139. doi:10.1017/S1743921322000588
7. M. Apetrii, A. Celletti, C. Efthymiopoulos, C. Gales, T. Vartolomei, On a simulator of break-up events for space debris, Sumbitted to CMDA (2023)

Thank you for your attention!

Email: *tudor.vartolomei@uaic.ro*